

## Robust Advanced PID Control (RaPID) PID Tuning Based on Engineering Specifications

JAIRO J. ESPINOSA OVIEDO, TOM BOELEN, and PETER VAN OVERSCHEE

The success of proportional-integral-derivative (PID) control in the process industry is based on the ability to stabilize and control around 90% of existing processes [1]. This importance is overshadowed, however, by a lack of performance in some applications. It has been reported that a significant percentage of installed PIDs are operated in manual mode and that 65% of the loops operating in automatic mode generate greater variance in closed-loop operation than in open-loop operation [1], [2]. This lack of performance is, in many cases, the result of a poorly tuned set of parameters due to

- » lack of knowledge among operators and commissioning personnel
- » generic tuning methods based on ad hoc criteria that do not match specific process needs
- » the large variety of PID structures, which leads to errors during application of tuning rules.

These challenges motivated our development of the software package Robust Advanced PID Control (RaPID) for tuning PID controllers. RaPID is an intuitive tool with multiple levels of complexity that can be accessed according to the knowledge of the person commissioning the loop. This article describes the methods and algorithms used by RaPID for tuning PID loops.

### PROJECT DESCRIPTION

In the project description, the user provides information about the control loop, such as sampling time, ranges, units, names, and descriptions of the setpoints, the controlled variable, and the manipulated variable. These definitions are needed to interpret sampled data and define the limits of variables. The limits provide saturation constraints as well as appropriate scaling of variables.

In this phase of the project, the user defines the objective that must be achieved once the PID is tuned (either disturbance rejection or setpoint tracking) as well as the template of the controller. The template of the controller contains the parameter format, which can be selected for several different commercial PID controllers as stand-alone units or integrated in distributed control system (DCS) units. The templates are based on the description provided by the manufacturers, which include Siemens, Emerson, Omron, Honeywell, and others. The templates provide two benefits: 1) exact knowledge of the controller structure to maximize the performance of the controller hardware and 2) elimination of the need for manual conversion of the controller parameters from the traditional  $K_p$ ,  $T_i$ , and  $T_d$  to the manufacturer's format. This conversion reduces errors due to scaling and entering parameters.

The interface also allows the user to employ engineering units rather than scaled values.

### COLLECTION OF PROCESS DATA

Once the elements of a project have been decided, RaPID uses an input-output experiment to identify the dynamics of the plant. Experiments are costly because they interrupt normal plant operations. To minimize the impact of experiments, RaPID determines a set of inputs that can be chosen according to the present conditions and the features of the process by adjusting parameters such as amplitude and dc content. The available predefined input signals include step-like (step, block, polynomial step, and saturated ramp), impulse, sine wave (including single sine, swept sine, and multisine), and noisy inputs, namely, random Gaussian and pseudorandom binary noise sequence (PRBNS). Users can also create custom input signals.

Signals generated during the experiment can be loaded into the program by means of files or by using an object linking and embedding for process control (OPC) connection to the process computer. The OPC connection provides a reading and writing connection by which the manipulated variable (input) signal for the experiment can be designed in RaPID and sent to the DCS through OPC. The controlled variable signal is then read back and used for the identification.

### IDENTIFICATION

RaPID includes a system-identification algorithm that combines subspace identification and prediction error methods [3], [4], complemented by an intuitive user interface (see Figure 1). Once the signals from the experiment are acquired, RaPID sweeps over a set of structures to test models with different delays and numbers of poles and zeros. The model with the best fit is automatically selected. The algorithm detects integral effects and applies automatic preprocessing to remove signal offset. Advanced options include signal filtering using lowpass, highpass, bandpass, and bandstop filters. These filters can be configured by selecting the cutoff frequencies and the dynamic order. All changes can be previewed prior to being applied.

The user can also set the maximum delay and the maximum number of poles and zeros. In many cases, the operator has a good idea of the dc gain of the process. This prior knowledge can be used by limiting the dc gain of the model. During identification, the user can restrict the

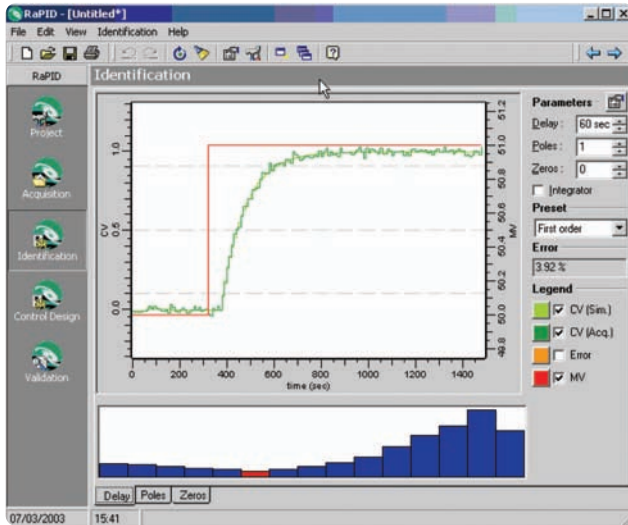


**FIGURE 1** Identification panel of RaPID. The dark green signal is the measured signal (output), the light green signal is the identified model output, and the red line is the manipulated variable (input). The tool calculates a set of models with different structures in terms of poles, zeros, and delays and automatically selects the model structure with the best performance. The user can select options by combining this result with prior knowledge about the process.

presence of resonant poles as well as imaginary and right-half plane zeros. The user can test different models with a single click, and the model can be evaluated graphically by comparing the simulated response with the real response or numerically by calculating an error index, which measures the portions of the output signal that are not correctly explained by the model.

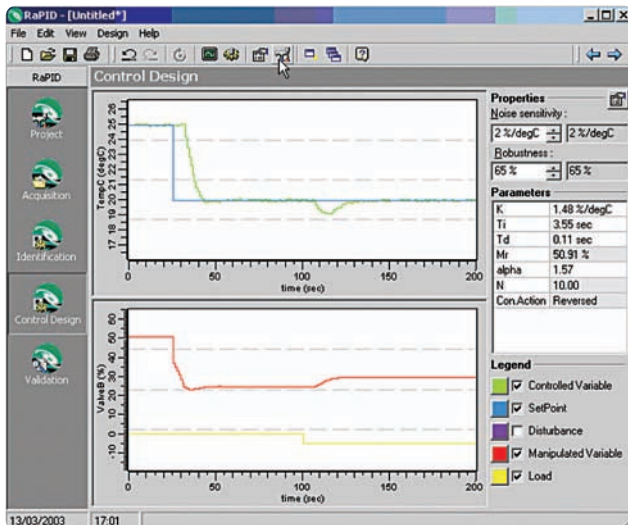


**FIGURE 2** User interface for controller optimization. “Properties” allows the user to define constraints on noise sensitivity (HF gain) and robustness. The calculated controller is presented according to the definitions of the PID controller template. The resulting robustness and noise sensitivity are shown. The user can define the conditions of the test, such as setpoint, disturbance, and load changes.

Although all models are identified as discrete-time systems, the results are shown in a continuous representation, which is more intuitive to the user.

## CONTROL DESIGN

PID controllers have traditionally been tuned by prescribing the shape of the closed-loop step response (Ziegler-Nichols, Chien-Hrones-Reswick, and Cohen-Coon [1], [2]). After the parameters are found according to the method, a trial-and-error approach is used to achieve the desired response, often sacrificing the robustness provided by the original parameters.

For controller design, RaPID uses constrained optimization to obtain the desired time response while guaranteeing robustness. Three elements must be defined: control objective and control structure, cost function, and constraints. Selection of the optimization criterion (cost function), control objectives, and constraints can be done through the user interface as shown in Figures 2 and 3. The user interface allows interactive design of the controller, including reformulation of the objectives and constraints. These elements are described in the following sections.

### Control Objective and Control Structure

The control objective is chosen by the user according to the application. Objectives that can be pursued with RaPID include

- » tracking, that is, following a prestored or real-time reference signal (servomechanism problem)
- » variance control, that is, keeping the output of the system at a setpoint while recovering as quickly as possible from disturbances (regulator problem).

To achieve these objectives, RaPID optimizes the PID parameters  $K_P$ ,  $K_I$ ,  $K_D$ , and  $K_{DD}$ , as well as the parameters  $\alpha$ ,  $\beta$ , and  $\gamma$  of the feedforward action, where the controller is represented by

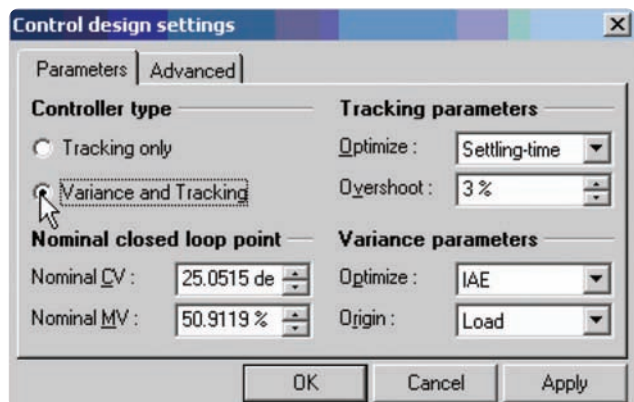


**FIGURE 3** User interface for controller optimization. This window defines the control objectives, cost function, and overshoot constraints. The origin of the variance change is defined by setting the source either as a load or as an output disturbance. The nominal operating point is described in the entries Nominal CV (controlled variable) and Nominal MV (manipulated variable). The cost function can be selected as either IAE, ITAE, or energy.

$$\begin{aligned}
 U(s) = & K_P(\alpha R(s) - Y(s)) + \frac{K_I}{s}(R(s) - Y(s)) \\
 & + K_D \frac{s}{s + P_d}(\beta R(s)Y(s)) + K_{DD} \frac{s^2}{(s + P_d)^2}(\gamma R(s) - Y(s)) \\
 & + \text{manual reset.}
 \end{aligned} \tag{1}$$

A block diagram of the controller (1) is shown in Figure 4. Table 1 outlines the function of each controller element for the different control objectives. For instance, when the control objective is tracking, the feedback and feedforward parameters are both optimized. On the other hand, when the objective is to simultaneously achieve tracking and variance control, the feedback parameters are employed for variance control while the feedforward parameters are targeted to the tracking objective.

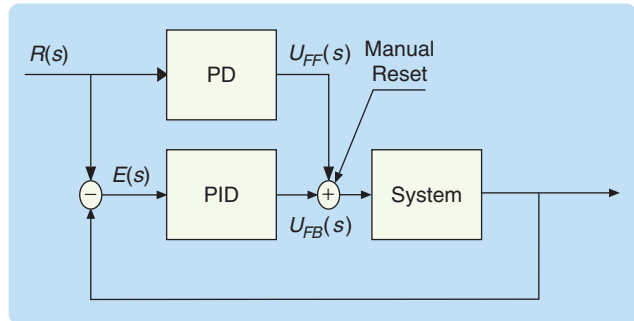


**FIGURE 4** PID control with feedforward PD action and manual reset. The feedforward action is used only for tracking applications. The manual reset is a constant value added to the control action to guarantee bumpless transfer of the controller from manual to automatic.

### Optimization Criteria

Once the control objective and the structure (template) of the controller have been selected, the next step in tuning is to select criteria to evaluate the controllers during optimization. For optimization, RaPID uses time-defined criteria and overall error criteria. For a time-defined criterion, the optimization minimizes the time needed to reach a given point of the step response. RaPID includes both settling time and rise time as time-defined criteria.

Alternatively, an overall error criterion evaluates the error signal over a period of time ( $N$  samples) in response to a step reference (see Figure 5). The idea is to capture in a single number the total deviation between the reference and the output of the system. The overall error criteria used by RaPID are

- 1) integral of absolute error (IAE)

$$IAE = \sum_{k=1}^N |e_k|$$

- 2) energy  $E = \sum_{k=1}^N e_k^2$

- 3) integral of time multiplied by the absolute value of error (ITAE)

$$ITAE = \sum_{k=1}^N k|e_k|.$$

### Optimization Constraints

Optimizing the parameters of the controller based only on the optimization criteria often results in a controller with less than satisfactory behavior. RaPID thus includes various constraints.

**TABLE 1** Controller functions for achieving the control objectives. When the control objective is tracking, the feedback and feedforward parameters are both optimized. On the other hand, when the objective is to achieve both tracking and variance control, the feedback parameters focus on the variance while the feedforward parameters aim at the tracking objective.

Controller Section	Controller Objective		
	Tracking	Variance	Variance + Tracking
Feedback	Tracking mode	Variance mode	Variance mode
Feedforward	Tracking mode		Tracking mode

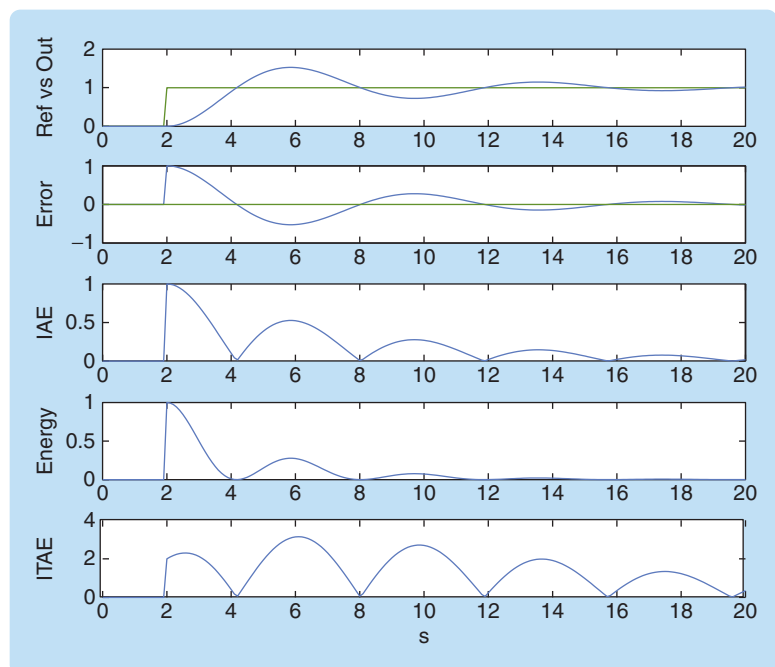


**FIGURE 5** Error-based optimization criteria. The top plot shows a reference signal and the controlled variable of the system. The error plot shows the tracking error from the reference, calculated as the difference between the reference and the output. The last three plots show instantaneous values of the signals used to calculate the performance of the controller. Observe that the IAE criterion penalizes proportionally to the absolute value of the error, the energy criterion penalizes according to the square of the error (large errors are strongly penalized compared with small errors), and the ITAE criterion penalizes “late” errors.

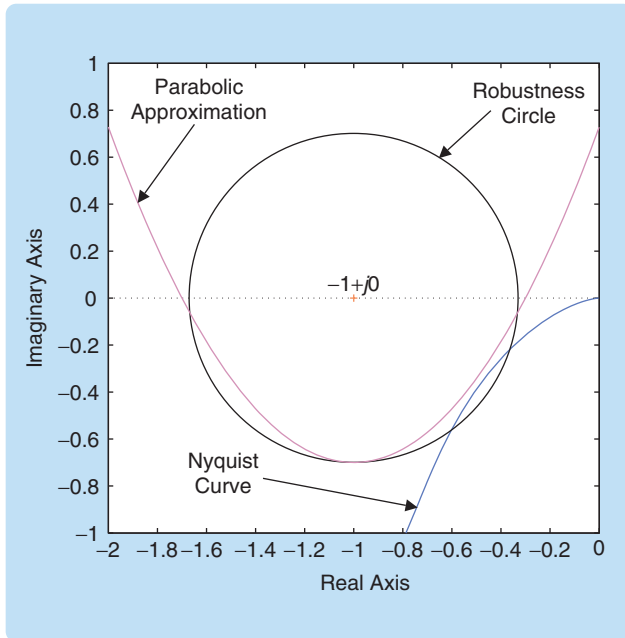


**FIGURE 6** Nyquist plot and the parabolic robustness constraint. During controller optimization, the robustness constraint (black) is approximated by a parabola (magenta), which passes through the intersection points of the robustness circle with the real axis. This constraint guarantees robustness and stability of the system with the optimized PID controller.

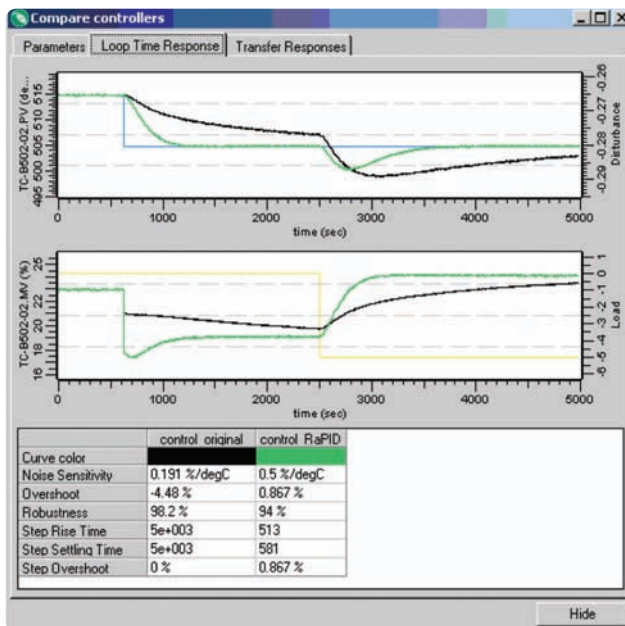


**FIGURE 7** User interface for controller comparison. The user interface shows the closed-loop simulation response of the controller with the original PID settings (black) and the PID settings obtained with RaPID (green). The upper figure shows the controlled variable and the reference while the lower plot shows the manipulated variable and the load disturbance. The figure shows a test in which the setpoint (blue) is changed at time 600 s; once the plant has reached this setpoint a load disturbance is applied (yellow). The table provides a numerical comparison of various performance measures for the controllers.

### Overshoot

This constraint allows the user to specify the maximum permissible overshoot. This constraint can be invoked only for the tracking control objective.

### Saturation

The saturation constraint restricts the actions of the controller to the actuator's physical limits, thus avoiding integrator windup, which can result in poor performance or instability.

### High-Frequency Gain

This constraint on the controller gain limits the effects of the high-frequency measurement noise on the actuator. Selecting the maximum high-frequency gain (HF-Gain) provides a trade-off between the speed of the controller and its sensitivity to noise. When HF-Gain is selected to be too small, the controller reacts slowly in tracking and variance control.

### Robustness

RaPID can guarantee robust stability and performance of the optimized PID values through a robustness constraint. Specifically, RaPID uses a parabolic constraint to prevent the Nyquist curve from encircling the -1 point. Figure 6 illustrates the parabolic constraint, while Figure 7 compares the performance of an initial PID controller with a PID controller optimized by RaPID.

## CONCLUSIONS

RaPID has been applied to hundreds of PID loops ranging from mechanical systems to process control loops and embedded applications. Power plants, refineries, chemical plants, and food and beverage plants are just a few of the applications that have benefited from this methodology.

RaPID enhances stability and safety in plant operation while improving productivity. We believe that the robustness of the controllers is the most likely explanation for the success of RaPID. Reduction in down times due to actuator failures has also been observed. This reduction can be explained by the limitation of the influence of sensor noise on the control actions, thanks to the constraint on the HF-Gain of the controller made possible by optimization. Energy savings and increased production have also been reported; these improvements are likely due to better tuning for variance control.

## AUTHOR INFORMATION

Jairo J. Espinosa Oviedo (Jairo.Espinosa@ipcos.be) obtained his electronics engineering degree from the Universidad Distrital de Bogotá, Colombia, and master's (cum laude) and Ph.D. (magna cum laude) degrees in electrical engineering from the Katholieke Universiteit Leuven, Belgium. He is currently a research and development engineer for IPCOS N.V. in Leuven, Belgium. He combines his work at IPCOS with teaching assignments at the Universidad de Ibagué in Colombia. He is the author of *Fuzzy Logic, Identification and Predictive Control*.

Tom Boelen received his M.Sc. in agricultural engineering in 1997 from the Katholieke Universiteit Leuven. He was a researcher in the field of biological process technology at the same university. He joined ISMC in 1998 and is currently a project engineer for projects in the chemical and petrochemical industry.

Peter Van Overschee received his M.Sc. degree in applied sciences in 1989 at the Katholieke Universiteit Leuven, Belgium. In 1990 he received his M.Sc. degree in electrical engineering at Stanford University, California. In 1996 he received the *Automatica* Best Paper Award. He is president of IPCOS Belgium and is responsible for projects in the oil industry.

## REFERENCES

[1] A. O'Dwyer, *Handbook of PI and PID Controller Tuning Rules*. London: Imperial College Press, 2003.

[2] K. Aström and T. Haggglund, *PID Controllers: Theory, Design and Tuning*. Research Triangle Park, NC: Instrum. Soc. Amer., 1995.

[3] L. Ljung, *System Identification—Theory for the User*. Englewood Cliffs, NJ: Prentice-Hall, 1999.

[4] P. Van Overschee and B. De Moor, *Subspace Identification for Linear Systems*. Norwell, MA: Kluwer, 1996.

[5] *Rapid, Robust advanced PID control. Course Control Theory Hands on Tuning and Application*, Leuven: IPCOS N.V., 2004.

[6] G.F. Franklin, J.D. Powell, and M.L. Workman, *Digital Control of Dynamic Systems*. Reading, MA: Addison-Wesley, 1990.

[7] F.G. Shinskey, *Process Control Systems, Application, Design and Tuning*. New York: McGraw-Hill, 1996.

[8] P.B. Deshpande, *Multivariable Process Control*. Research Triangle Park, NC: Instrum. Soc. Amer., 1989.

[9] P. Friedman, *Economics of Control Improvement*. Research Triangle Park, NC: Instrum. Soc. Amer., 1995.

[10] M. Morari and E. Zafiriou, *Robust Process Control*. Englewood Cliffs, NJ: Prentice Hall, 1999.

## Precision Timing Control for Radioastronomy Maintaining Femtosecond Synchronization in the Atacama Large Millimeter Array

JEAN-FRANÇOIS CLICHE and BILL SHILLUE

The Atacama Large Millimeter Array (ALMA) (see Figure 1) is an international radio astronomical facility currently under construction in Chile through the collaboration of institutions in the United States, Canada, Europe, and Japan [1]. When completed, the facility will consist of an array of up to 64 12-m parabolic antennas that can detect millimeter and submillimeter wavelength radio waves in the frequency band between 31–950 GHz. The antenna will be located at an elevation of 5,000 m on the Chajnantor plain in the district of San Pedro de Atacama. At these wavelengths, the radiotelescope array will be able to reveal the structure of the cold regions of the universe, otherwise dark at visible wavelengths, with unprecedented sensitivity and a resolution of 10 milliarcseconds. This resolution is an order of magnitude better than the Hubble telescope or the very large array operating in New Mexico.

ALMA achieves its exceptional resolution and sensitivity by linking all of the 64 antennas into an interferometer array. In this setup, the exact instant at which a radio wave reaches each of the antennas is precisely recorded. Since the relative position of each antenna is well known, the source of the wave can be accurately pinpointed by comparing the timing (or phase) of the wave arriving at any one antenna relative to the other antennas using real-time correlator systems. The distance between two antennas is known as the baseline. A large baseline causes signals to arrive at the antennas with a large differential delay, and thus accurate angular resolution can be achieved. The ALMA antennas can be moved into different configurations like chess pieces using a specially designed truck to achieve different combinations of resolution and sen-

sitivity. The maximum resolution is obtained with baselines up to 18 km.

To accurately measure the phase of the sky signal over the entire array or subarray, every antenna must receive a highly stable common reference signal known as the local oscillator (LO) reference. For ALMA, this LO reference signal is composed of two optical waves sent through a single optical fiber [2]. Both waves have a wavelength around 1.556  $\mu\text{m}$  to allow transmission through conventional telecommunication optical fiber with little loss. One optical wave is generated by a master laser (ML), while the other is generated by phase-locking a slave laser at a given frequency offset from the master. Both



**FIGURE 1** Artist's rendition of the ALMA radiotelescope, which will consist of up to 64 12-meter parabolic antennas spread over 18 km. The array will receive cosmic signals from 31–950 GHz. Image courtesy of NRAO/AUI and computer graphics by ESO.